



Monolayer solid of N-2/Ag(111)

Bruch, L.W.; Hansen, Flemming Yssing

Published in:
Physical Review B

Link to article, DOI:
[10.1103/PhysRevB.57.9285](https://doi.org/10.1103/PhysRevB.57.9285)

Publication date:
1998

Document Version
Publisher's PDF, also known as Version of record

[Link back to DTU Orbit](#)

Citation (APA):
Bruch, L. W., & Hansen, F. Y. (1998). Monolayer solid of N-2/Ag(111). *Physical Review B*, 57(15), 9285-9292.
<https://doi.org/10.1103/PhysRevB.57.9285>

General rights

Copyright and moral rights for the publications made accessible in the public portal are retained by the authors and/or other copyright owners and it is a condition of accessing publications that users recognise and abide by the legal requirements associated with these rights.

- Users may download and print one copy of any publication from the public portal for the purpose of private study or research.
- You may not further distribute the material or use it for any profit-making activity or commercial gain
- You may freely distribute the URL identifying the publication in the public portal

If you believe that this document breaches copyright please contact us providing details, and we will remove access to the work immediately and investigate your claim.

Monolayer solid of $N_2/Ag(111)$

L. W. Bruch

Department of Physics, University of Wisconsin-Madison, Madison, Wisconsin 53706

F. Y. Hansen

Department of Chemistry, Technical University of Denmark, IK-207-DTU, DK-2800, Lyngby, Denmark

(Received 21 October 1997)

An incommensurate monolayer solid of $N_2/Ag(111)$ is modeled using extensive molecular-dynamics simulations. The conditions treated range from the low-temperature orientationally ordered solid to the melting of the solid. The properties are evaluated as a function of spreading pressure. Comparison is made to recent experimental data for $N_2/Ag(111)$ and to results for N_2 adsorbed on graphite, Cu(110), and MgO(001). [S0163-1829(98)02715-5]

I. INTRODUCTION

Phenomena reflecting the competing effects of adsorbate-adsorbate and adsorbate-substrate interactions are prominent in the physical adsorption of small molecules and have been studied most extensively for nitrogen. Changes in the monolayer relative to the three-dimensional (3D) solid¹ include (i) differences in the intrinsic geometry from packing in a plane rather than in 3D, (ii) changes in center-of-mass geometry driven by commensurate and near-commensurate lattices of the monolayer on the substrate, and (iii) differences in the character of the superlattice of orientationally ordered molecules. Besides these structural effects, there also are qualitative changes in the sequence of disordering transitions as the temperature is increased, from orientational order to disorder and from solid to dense fluid ("liquid") to dilute fluid ("gas"). In most of the systems studied the effects of (i), (ii), and (iii) are so entwined that it is difficult to appraise them separately, although computer simulations have enabled some comparisons of corrugated and smooth surface models. Adsorption of inert gases on Ag(111) provided information on systematic trends for the intrinsic 2D solids of monatomic adsorbates, with no apparent effects of the atomic discreteness of the substrate.² Recent measurements³ for $N_2/Ag(111)$ also show no commensurate structures and raise the prospect that comparisons with solids of N_2 adsorbed on graphite, Cu(110), and MgO(001) may help to separate the effects. The purpose of this paper is to report and discuss computer simulations of the $N_2/Ag(111)$ system that explore how much of the recent data can be understood with a model of adsorption on a structureless 2D surface and also what phenomena might become accessible with extensions of the experiments.

The phase diagram of monolayer N_2 /graphite is the most completely characterized case in molecular physisorption⁴ and presents the remarkable feature that there is *no* 2D triple point coexistence of solid, liquid, and gas. The submonolayer commensurate solid melts at ≈ 48 K, which correlates better⁵ with an estimate of the critical temperature of Lennard-Jones atoms than of the intrinsic 2D triple point temperature of ≈ 35 K. Apparently, the substrate corrugation stabilizes the solid to higher temperatures than the intrinsic triple point. On

an uncorrugated surface, the melting of the monolayer N_2 solid might occur at temperatures closer to 35 K. Further, the melting temperature of commensurate N_2 /graphite increases from 48 K to 75 K as the coverage increases from 0.5 to 1.0 ML; the increase has been discussed in terms of changing mechanisms of vacancy production. At least part of the increase can be attributed to the increase of melting temperature with (2D) spreading pressure, but there has been no systematic analysis of the effect for a molecular solid. This paper includes calculations for smooth N_2 /graphite to illustrate the pressure effect and for comparison with smooth $N_2/Ag(111)$.

The low-temperature solid of monolayer N_2 /graphite is orientationally ordered in a two-sublattice herringbone structure and disorders at 26–28 K. The corresponding transition has not been observed³ for $N_2/Ag(111)$, and the question arises as to whether this is because the experiments were not carried to low enough temperatures or because no superlattice is formed of the ordered molecular axes, as appears to be the case for $N_2/MgO(001)$ (Ref. 6) and $N_2/Cu(110)$.⁷ A related issue is "how spherical" the N_2 molecule in the orientationally disordered state is and how large a distortion there is from the triangular lattice of spherical molecules. The center-of-mass lattice of $N_2/Ag(111)$ at $T > 25$ K is apparently a triangular lattice,³ as for inert gases on Ag(111), and it is of interest to see the extent to which that is reproduced by a simulation.

The molecular-dynamics simulations reported here are in some ways a simplified version of an extensive set of computations⁸ for commensurate N_2 /graphite. Effects of atomic discreteness of the substrate and of electrostatic fields arising from substrate charge distributions are neglected. However, because the center-of-mass lattice is derived from the simulation, rather than input to it, the required volume of computation is very large. Also, the model⁹ of the molecule-substrate interaction is more primitive than for N_2 /graphite because of the absence of adsorption isotherm data and inelastic scattering data.

The organization of this paper is as follows. Section II contains the formulation of the calculations and analysis. Section III contains results for the monolayer solid of

N₂/Ag(111) and some results for N₂ on flat graphite. Section IV contains a discussion.

II. INTERACTION MODEL AND SIMULATION METHODS

The simulations correspond to a smooth surface (no corrugation) version of calculations performed⁸ for N₂/graphite. Indeed, a parallel series of calculations was performed for the graphite case with the corrugation terms set equal to zero, and the results are discussed in Sec. IV E. In the present work, the N₂-N₂ interactions are the same as for N₂/graphite, but the N₂-substrate and substrate-mediated dispersion energy terms differ.

A. Molecule-substrate interaction

The molecule-substrate potential $V(\mathbf{r})$ is taken to be an atom-atom sum of Morse potentials with parameters set by Tully and co-workers,⁹

$$\phi(r) = D[\exp\{-2\alpha(r-r_0)\} - 2\exp\{-\alpha(r-r_0)\}], \quad (2.1)$$

with $D = 5.2$ meV, $r_0 = 3.8$ Å, and $\alpha = 1.2$ Å⁻¹. The one-molecule adsorption energy (with zero-point energy term) obtained by summing over the top two layers¹⁰ of the Ag(111) surface is 79 meV, with perpendicular vibration frequency $\omega_{\perp} = 4.7$ meV. The energy/molecule in the quasiharmonic ground state of the monolayer is 96–99 meV, depending on which combination of substrate-mediated energy terms is included. For comparison, the experimental heat of adsorption at monolayer condensation is $q_1 = 103 \pm 4$ meV.³

At low temperatures and low spreading pressures, the modeling of the monolayer phase diagram is insensitive to the precise value of the energy minimum but effects of molecular tipping relative to the surface plane depend on the curvature at the minimum. One piece of information supporting the value of ω_{\perp} in the N₂/Ag(111) model is that a scaling of ω_{\perp} for N₂/graphite (~ 6.2 meV, from inelastic neutron scattering¹¹) in analogy to the corresponding values¹² for adsorbed Kr gives an estimate of 4.2 meV. The N₂/Ag(111) model used here has the property that tipping of the N₂ axis relative to the surface plane requires less energy for Ag(111) than for graphite. However, there has been a suggestion,¹³ based on electron energy-loss spectroscopy, that the frequency should be in the range 6–9 meV and hence that the ordering is reversed. Inelastic helium scattering from the N₂/Ag(111) could determine ω_{\perp} and provide a basis for an improved model.

For the monolayer simulations the uncorrugated version of this model is used. Only the laterally averaged holding potential¹⁴ $V_0(z)$ is retained. This approximation is made both because of the absence of registry structures in the experiments³ and because the use of atom-atom sums to estimate the potential energy corrugation for a monolayer on a close-packed metal surface is known to be unreliable.^{14,2} The lattice constants in the LEED experiment for N₂/Ag(111) have a large misfit relative to low-order commensurate structures, similar to the case of Kr/Ag(111), which has been modeled with a smooth substrate.

The parameters of the substrate-mediated (McLachlan) dispersion energy² are $C_{s1} = 46.4$ au and $C_{s2} = 32.0$ au and the overlayer distance is taken relative to the ideal jellium edge, $L_{ov} = z - (d/2)$ with $d = 2.36$ Å for Ag(111). Effects of dielectric screening of the static N₂ quadrupole moment (“static image terms”) are neglected.

B. Computations

The calculations are performed with an isothermal (constrained) molecular-dynamics algorithm¹⁵ in which the N-N bond distance is fixed at its equilibrium value of 1.098 Å. Periodic boundary conditions in directions parallel to the surface plane are used and there are 224 molecules in the monolayer film. This is a classical mechanics approximation and is applied at temperatures down to 15 K; a quasiharmonic lattice dynamics approximation¹⁶ is used to estimate the size of quantum corrections at the lowest temperatures. The molecular-dynamics technique is essential for treating the experimental conditions of a molecular solid with disordered azimuthal angle of the N-N bond. The low temperature orientationally ordered solid requires a more extensive search for the minimum-energy structure than for commensurate N₂/graphite. In both the molecular-dynamics and the quasiharmonic calculations, the search is made in the context of a rectangular unit cell [$= 14 \times 16$ molecules in the simulation] and yields two-sublattice herringbone ordering. The sides of the unit cell have ratio $L_1/L_2 = \sqrt{3}$ when the center-of-mass lattice is a triangular lattice. On a smooth surface, the aspect ratio of the herringbone cell differs from $\sqrt{3}$ and is 5% smaller at the lowest temperature (15 K) in this work. The main indicator for the 2D solid is the static structure factor evaluated at wave vectors corresponding to the average center-of-mass lattice.

The spreading pressure in the molecular dynamics work is evaluated from the virial theorem¹⁷ for separate dilations of the two sides of the rectangular cell. Two diagonal elements of the stress tensor ϕ_{xx} and ϕ_{yy} are evaluated and provide a diagnostic of a trend to herringbone ordering. In the orientationally disordered solid, where the molecular projection on the plane is approximately a disk, one expects $\phi_{xx} \approx \phi_{yy}$ in a triangular lattice. At low temperatures, the triangular center-of-mass lattice with orientational ordering has $\phi_{xx} \neq \phi_{yy}$.¹⁸ Departures from equality of the diagonal components of the stress tensor are used to estimate the extent to which the equilibrium lattice might be distorted from triangular. The search for an unconstrained monolayer solid becomes a matter of adjusting the cell sides L_1 and L_2 until $\phi_{xx} = \phi_{yy} = \bar{\phi} = 0$.

C. Thermodynamic characterizations

The isothermal bulk modulus of the monolayer can be obtained from measurements along an isotherm,

$$B_T = -A \left. \frac{\partial \bar{\phi}}{\partial A} \right|_T, \quad (2.2)$$

for area/molecule A . It can also be derived² from measured isobaric thermal expansion coefficients³ and the isosteric heat q_{st} using

$$B_T = q_{st} / [\sqrt{3}L(\partial L/\partial T)|_p], \quad (2.3)$$

where L is the lattice constant of a triangular solid. A comparison of such empirical values with values derived from the simulations provides a rough test of the equation of state of the monolayer solid.

Maxwell relations provided a consistency test for the calculations. The isothermal derivative of the internal energy is

$$\left. \frac{\partial E}{\partial A} \right|_T = T \left. \frac{\partial \bar{\phi}}{\partial T} \right|_A - \bar{\phi}. \quad (2.4)$$

Thus E need not be a monotonic function of A . The virial pressures and their temperature derivatives were consistent with the location of zeroes of $(\partial E/\partial A)|_T$.

The form of phase transition phenomena in these simulations¹⁹ corresponds to those in an N - A - T ensemble. For instance, the evolution of the system along an isochore with increasing temperature is from (i) solid to (ii) solid-liquid coexistence along the melting line to (iii) liquid. The spreading pressure as a function of temperature has three distinct approximately linear segments along such an isochore, with slopes S_1 , S_2 , and S_3 respectively, as in Fig. 1(a). The slopes are related by $S_3 < S_1 < S_2$. Confirmation of the inferred one- and two-phase character of these regimes is provided by molecular trajectory plots. Correlating the two-phase segments for different isochores leads to an estimate of the slope of the melting curve $d\phi/dT|_{\text{melt}} = \Delta S/\Delta A$. Then, using the bulk modulus, the difference ΔA in molar areas of liquid and solid at coexistence is obtained, and hence the entropy change ΔS at melting can be estimated. As in most 2D simulations,² the melting appears to be first order.

The orientational order-disorder transition of $N_2/\text{graphite}$ and the corresponding α - β transition of 3D N_2 are both weakly first order.^{1,4} In these simulations, the structure factor of the leading herringbone diffraction line decreases to zero as the temperature increases from 15 to about 20 K. However, the precision in the calculations is insufficient to decide whether the transition is first or second order. The cell-side lengths are incremented by about 1% in the searches. The discontinuity in molar volume for 3D N_2 is¹ 1.4%, equivalent to about 1% in area. To make a definitive assignment of the order of the transition will require a finer grid of cell sizes, more thorough averaging of fluctuations (longer simulation times) and larger simulation cells. The present state of the interaction model does not appear to warrant such a large computational effort.

III. MONOLAYER SOLID

The calculations were done for models denoted $X1M$ and $X1$, respectively, that included or omitted the McLachlan energy; $X1$ is the designation of the 3D N_2 - N_2 pair potential. The mechanism of the substrate-mediated dispersion force should apply for molecules as it does for inert gases.² However, the results here show, in accord with experience for $N_2/\text{graphite}$ ^{5,20} and for $O_2/\text{graphite}$,²¹ that the $X1$ model follows the experimental lattice constants and the domain of existence of the 2D solid³ somewhat better.

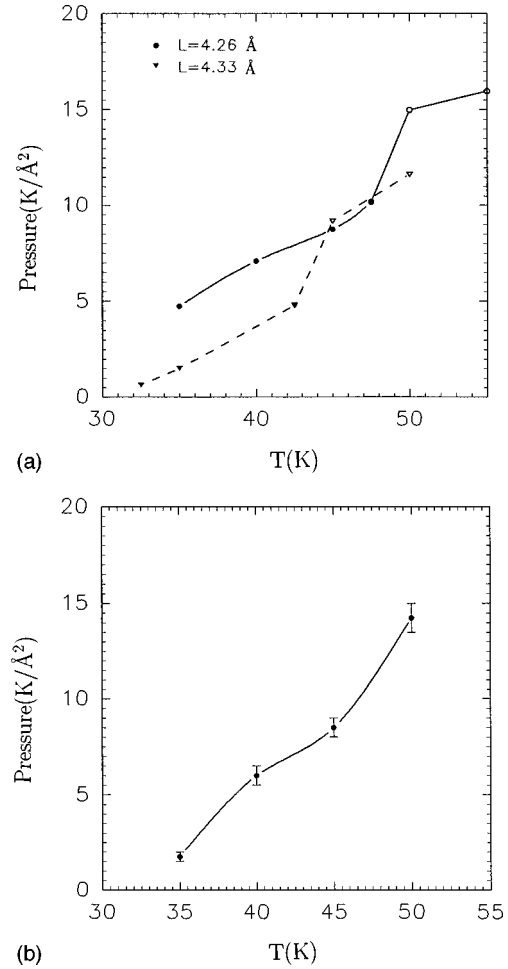


FIG. 1. Spreading pressure as a function of temperature for two isochores and the melting transition. $\bar{\phi}$ (in $\text{K}/\text{\AA}^2$) is shown as a function of T (in K) for the $X1M$ model of $N_2/\text{Ag}(111)$. (a) Isochores corresponding to triangular lattices with L equal to 4.26 \AA and 4.33 \AA ; filled symbols denote states in which the film is primarily crystalline, open symbols states in which the film is fluid. (b) Melting pressure as a function of temperature obtained from the onset of van der Waals loops in isotherms such as those shown in Fig. 2(b). The lines between plotted points are included only to guide the eye and contain no information beyond the data shown.

A. Benchmarks

Solutions at 15 K for the $X1M$ solid at zero spreading pressure can be compared for a measure of the contributions of quantum effects and thermally activated disorder. The molecular-dynamics solution is classical and has a rectangular cell $7.1 \times 4.36 \text{ \AA}^2$ with average energy -1142 K/molecule and area $15.5 \text{ \AA}^2/\text{molecule}$. The $\hbar \rightarrow 0$ (classical) limit of the quasiharmonic approximation has a rectangular cell $7.09 \times 4.44 \text{ \AA}^2$ with average energy -1149 K/molecule and $15.8 \text{ \AA}^2/\text{molecule}$. The cell for the quasiharmonic approximation with quantum corrections is dilated by 2% relative to the $\hbar \rightarrow 0$ structure and is a rectangular cell $7.23 \times 4.51 \text{ \AA}^2$ with $16.3 \text{ \AA}^2/\text{molecule}$. The partial thermal orientational disorder present in the molecular-dynamics solution leads to an aspect ratio $L_1/L_2 = 0.94\sqrt{3}$ that is a little larger than for the quasiharmonic approximation.²² Overall, the use of a classical molecular

TABLE I. Isothermal bulk modulus for monolayer solids of N_2 , in $K/\text{\AA}^2$ at specified temperature T in Kelvin, area A in $\text{\AA}^2/\text{molecule}$ and spreading pressure $\bar{\phi}$ in $K/\text{\AA}^2$.

Model ^a	T	A	f^b	L^c	$\bar{\phi}$	B_T
Ag(111)/X1M	15	15.5	0.94	4.16	0	200
	17.5	15.5	0.96	4.19	0	188
	20	15.6	1	4.24	0	135
	35–40	14.8	1	4.13	~15	195
	35–40	14.6	1	4.10	~19	230
	50	16.0 ^e			~12.5	82
Ag(111)/X1	15	15.2	0.94	4.12	0	250
	17.5	15.2	0.95	4.14	0	190
	20	15.2	0.99	4.18	0	160
	35–40	14.8	1	4.13	~11	200
	35–40	14.6	1	4.10	~15	220
	35–40	14.8	1	4.13	~23	240
Graphite/X1M ^d	35–40	14.6	1	4.10	~28	260
	60	16.0 ^e			~20.5	105
	35–40	14.6	1	4.10		250
Ag(111) ^f	~60	~16				~80
BN ^g	30	~13				280
MgO(001) ^h						

^aSubstrate and notation whether model includes the McLachlan energy term (X1M) or omits it (X1). The precision of calculated B_T is ~10%.

^bThe aspect ratio of the rectangular unit cell is written as $L_1/L_2 = f\sqrt{3}$; $f=1$ denotes a triangular center-of-mass lattice. The area/mol is $A = f\sqrt{3}L_2^2/2$.

^cNearest-neighbor center-of-mass spacing in \AA . For the rectangular lattices, this spacing is $0.5\sqrt{L_1^2 + L_2^2}$.

^dCalculation with flat graphite, retaining only the lateral average V_0 of the holding potential.

^eCalculations for dense fluid at the stated average density.

^fDerived from LEED isobars of triangular monolayer solid, Ref. 3, assuming $q_{st} = 103$ meV.

^gFrom adsorption isotherms for N_2 /BN, Ref. 24 near 60 K; identification of density based on x-ray diffraction at 47 K (Ref. 25).

^hFrom LEED isobars for uniaxially compressed solids of N_2 /MgO(001), Ref. 23.

dynamics simulation seems to be a good approximation down to 20 K and to still be informative at 15 K.

The structures observed³ for N_2 /Ag(111) have area/molecule in the range 13.9–15.0 \AA^2 . In other physisorbed N_2 systems it is: 15.7 \AA^2 for commensurate N_2 /graphite (and 14.1 \AA^2 in the densest monolayer solid), 14.45 \AA^2 in a higher-order commensurate lattice⁷ of N_2 /Cu(110) and 12.8–14.4 \AA^2 for N_2 /Mg(001).⁶

The chemical potential increase from monolayer condensation to bilayer condensation along an experimental isobar shown in Ref. 3 is ≈ 300 K. The spreading pressures for the X1 model are consistent with compression of the monolayer to ≈ 4.05 \AA at 35 K without bilayer condensation, using the $\bar{\phi}A$ term of the enthalpy. The chemical potential balance for stability at the smallest observed lattice constants is more problematic for the X1M model.

B. 2D Bulk modulus

Table I contains the bulk moduli of monolayer N_2 for several thermodynamic states. Values calculated for the X1M and X1 models are presented, as are empirical values derived from isobars for N_2 /Ag(111) (Ref. 3) and N_2 /MgO(001) (Ref. 23) and isotherms for N_2 /BN.²⁴ Fluctuations in the molecular-dynamics averages lead to 10% uncertainties in the calculated B_T .

The calculations at $A = 14.6$ \AA^2 (triangular lattice with $L \approx 4.10$ \AA) are in good agreement with the bulk modulus derived from the LEED experiments, which probably has 10% uncertainty in the identification of the relevant isosteric heat. Although the calculated bulk modulus depends primarily on the N_2 - N_2 interactions, and only weakly on the N_2 -Ag potential, the differences between the X1M and X1 cases are not large enough for the experimental B_T values to be a strong discriminator between the two models. The bulk modulus is smaller (compressibility is larger) for the fluid states as a consequence of the lower density.

The similarity of the experimental bulk moduli of N_2 on several substrates reflects the transferability of the molecule-molecule interactions in physical adsorption.

The calculated spreading pressures for the monolayer solids above 25 K appear to be isotropic. That is, $\phi_{xx} = \phi_{yy} \pm 0.2$ $K/\text{\AA}^2$ in a series of triangular lattices, where the variation appears to be statistical fluctuations in the molecular-dynamic averaging. If the increment is assigned to a change in the aspect ratio of the cell from a triangular to a centered-rectangular lattice by uniaxial dilation, there would be a fractional change $\Delta L/L \sim 1 \times 10^{-3}$ along that axis. Thus, the orientationally disordered monolayer molecular solid has a triangular center-of-mass lattice to 0.1% tolerance. To tighten the limits further is not feasible at the present level of computation.

C. Orientationally ordered solid

The low-temperature solids of 3D N₂ and of monolayer N₂/graphite are orientationally ordered with transition temperatures of 35.6 K and ~ 28 K, respectively.⁴ No such transition was observed for N₂/Ag(111) down to³ 25 K. No systematic extinction of superlattice diffraction spots is seen⁷ for N₂/Cu(110) in the temperature range 17–32 K. No herringbone order is seen⁶ for N₂/MgO(001) down to 10 K. The absence of an orientational phase transition in the latter two examples may be a consequence of the frustration of herringbone ordering in unit cells with an odd number of molecules. Thus, the question arises what the character of the axially ordered low-temperature state of N₂/Ag(111) may be.

The simulations on rectangular cells of 224 molecules show two-sublattice herringbone²⁶ ordering in the low-temperature solid; parameters of the $\bar{\phi}=0$ structure are given in Table I. The structure has “2 in” ordering, with molecular axes parallel to the plane, and is manifest in a nonvanishing superlattice structure factor⁵ $S(1,2)$. The superlattice strength $S(1,2)$ goes to zero with increasing temperature. There is an inflection point in the plot of quadrupole energy per molecule at about the temperature where $S(1,2)$ vanishes. The transition temperature is between 17.5 and 20 K for the *X1M* model and just slightly above 20 K for the *X1* model.²⁷ As the temperature is increased towards the transition, the distribution of molecular tilt angles broadens, indicating that the mechanism for disordering of the molecular axes is similar to that seen in simulations of N₂/graphite.¹⁵

The orientationally ordered solid has a nontriangular lattice of the molecular centers of mass, with the departure from the $\sqrt{3}$ aspect ratio increasing with increasing order and lowered temperatures. Thus, in addition to the superlattice diffraction spots there should be a structural signature from the lattice distortion.

D. 2D sublimation curve and triple point

Another reference state is the monolayer at zero spreading pressure, the “unconstrained solid.”² This is expected to be a good approximation to the state of the solid at monolayer condensation below the 2D triple point. The calculated lattice constant of the triangular lattice at $\bar{\phi}=0$, derived from isotherms such as those shown in Fig. 2(a), is listed for temperatures from 20 K to $T_t(2D)$ in Table II. Trajectory calculations confirm that N₂ on a smooth graphite or Ag(111) surface is a normal triple point system with solid, dense fluid (liquid), and dilute (gaseous) phases.

The estimated $T_t(2D)$ of N₂ obtained from scaling the 3D triple-point 63 K (Ref. 1) by the ratio (0.4/0.7) of the triple point temperatures of 2D and 3D Lennard-Jones atoms² is 36 K. The calculated triple point of N₂/Ag(111) for the *X1* model is 35–37.5 K, and is close to this estimate. For the *X1M* model, the melting temperature is lowered by 5–7 K, on the scale of the decrement found in calculations for commensurate N₂/graphite.⁵

The LEED experiments reported in Ref. 3 tracked (3D) isobars with decreasing temperature, and 2D solid was observed already at temperatures above 38 K. The largest observed lattice constants were $L=4.15$ Å. However, the re-

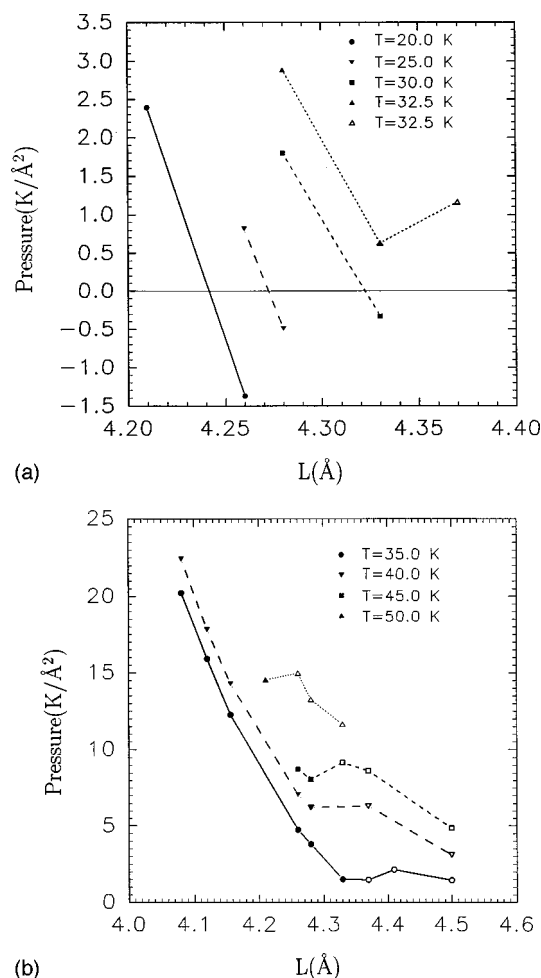


FIG. 2. Isotherms for the *X1M* model. The spreading pressure is plotted as a function of the equivalent triangular lattice spacing L . Filled symbols denote crystalline film states while open symbols denote fluid phase points. (a) Isotherms used to determine the zero-pressure lattices and the thermal expansion of the unconstrained solid. (b) Isotherms showing van der Waals loops and used to determine the melting-point curve in Fig. 1(b).

sults in Table I indicate that at such L values the system is under considerable spreading pressure. Also, the melting temperature variation for submonolayer N₂/graphite indicates that a lattice with $L=4.26$ Å is already under appreciable compressive stress. We therefore conjecture that the experiments crossed the melting curve of N₂/Ag(111), rather than its sublimation curve. One way to test this would be to determine structures of submonolayer solids of N₂/Ag(111) at $T < 30$ K.

These calculations imply that the melting of the monolayer solid is accessible to LEED experiments on N₂/Ag(111). This may be surprising considering that the melting of inert gas solids on Ag(111) occurs at temperatures and 3D pressures too high for LEED experiments. However, comparing the ratio of adsorbate-adsorbate potential minimum to the holding potential minimum on silver shows that the scaled lateral interactions are significantly weaker for N₂: ϵ/V_0 is 0.11 and 0.16 for N₂ and Kr, respectively.

E. 2D melting curve

The melting transition is identified in isochores and isotherms, which both show signatures of a first-order phase

TABLE II. Lattice constant of triangular monolayer solid of $N_2/Ag(111)$ at zero spreading pressure. Nearest-neighbor spacing L in Å and temperature T in K. $L(X1M)$ and $L(X1)$ denote values calculated with and without the McLachlan dispersion energy, respectively. The corresponding areas/mol are denoted $A(X1M)$ and $A(X1)$, in Å².

T	$L(X1M)$	$A(X1M)$	$L(X1)$	$A(X1)$
20	4.24	15.6	4.18	15.1
25	4.27	15.8	4.21	15.3
30	4.32	16.2	4.24	15.6
32.5	4.35 ^a	16.4		
35			4.27	15.8
37.5			4.30 ^b	16.0

^aMetastable solid; simulation shows formation of liquid at run times exceeding 500 ps. The unconstrained solid with $L \approx 4.33$ Å melts at 30–32.5 K.

^bMetastable solid; simulation shows formation of liquid at run times exceeding 500 ps. The unconstrained solid with $L \approx 4.28$ Å melts at 35–37.5 K.

transition. Along an isochore, as described in Sec. II C, the pressure appears to be piecewise linear as a function of temperature. Along isotherms, van der Waals loops appear once the triple-point temperature is exceeded. Some structures were metastable, with equilibration times of longer than 500 ps in the simulation. Figure 1 shows two isochores, with breaks in slope identified as melting transitions, and the melting curve inferred from the isotherms of Fig. 2. There are also breaks in slope at melting for the average height as a function of temperature. Examining the distribution of heights above the surface at a given coverage shows that this

break in slope is correlated with the promotion of a few molecules to a second layer, as in simulations for corrugated $N_2/graphite$,¹⁵ and that below the melting transition there is a strong broadening of the heights for first layer molecules indicating tipping of molecular axes out of the plane.

1. Monolayer on Ag(111)

The triple-point temperature determined by the onset of a van der Waals loop at nearly zero $\bar{\phi}$ is bracketed by $30 < T_i < 32.5$ K and $35 < T_i < 37.5$ K for the $X1M$ and $X1$ models, respectively. Although the experiments were carried to 40 K without a sign of the melting transition, this may be because the thermodynamic path corresponded to significant spreading pressure on the monolayer solid. The higher range for T_i in the second case is less at odds with the experiments.

The pressure dependence along two isochores, for $L = 4.26$ and $L = 4.33$ Å, is shown in Fig. 1(a). For the $L = 4.26$ Å case, the melting temperature is in the range 45–50 K. Direct simulations at 47.5 K gave a structure factor that was 15% lower than at 45 K but still one to two orders of magnitude larger than in the liquid phase at 50 K. This indicated that there might be coexisting regions of solid and liquid; confirmation of the interpretation was given by the trajectory plot shown in Fig. 3. If the limits of the two-phase region are taken to be at 47.5 and 50 K, the difference in area per molecule of the coexisting phases is $\Delta A/A \approx 5\%$ and the entropy difference is $\Delta S \approx 1.3k_B$. These values are in the range found in simulations of the melting of 2D inert gases.² The corresponding transition for the $X1$ model is in the range 50–55 K.

The 4.33 Å isochore showed several instances of metastable structures: solid and fluid phases were found to persist for hundreds of ps. The melting temperature is ≈ 40 K; at

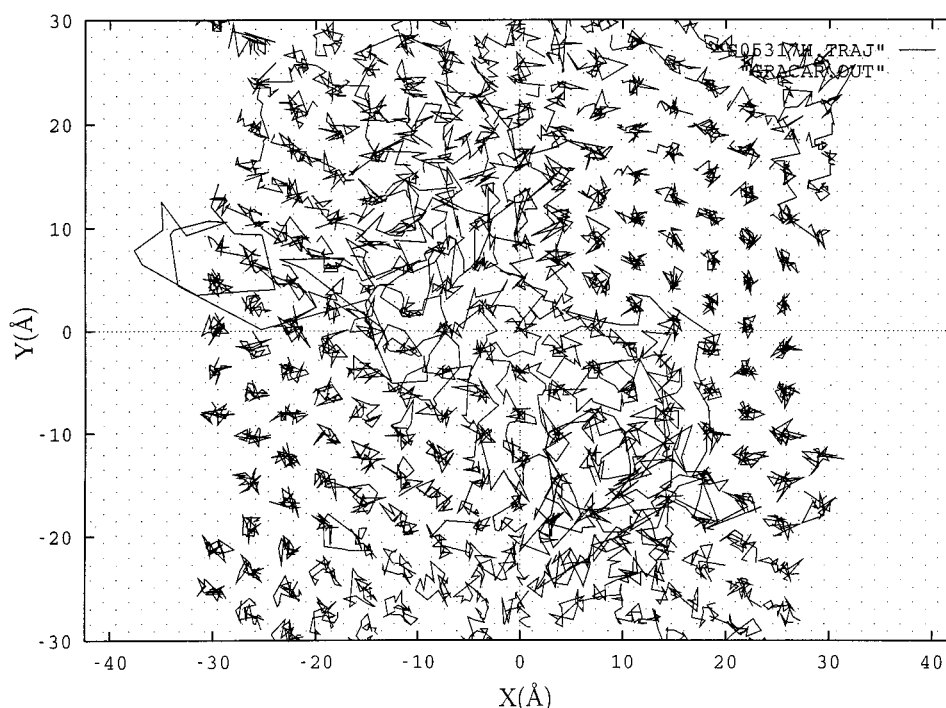


FIG. 3. Trajectory plot for the $X1M$ model at 47.5 K and with density corresponding to a triangular lattice with $L = 4.26$ Å. The trajectories of the N_2 centers of mass are shown for 100 ps following 800 ps equilibration time. Coexisting regions of crystalline solid and of fluid are present. The lines connect center-of-mass positions every 4.5 ps in the 100-ps time block.

42.5 K a trajectory plot showed disordered regions with mobile molecules, but some hexagonal ordering remained visible in those regions. The 4.33 Å lattice appears to be beyond the stability limit for the X1 model.

With either of the interaction models, the conclusion is that if the LEED experiments can be carried to 40 K, without too high a 3D gas pressure, the monolayer melting should be evident in the equivalent of a single crystal geometry rather than a powder pattern.

2. Monolayer on flat graphite

The case of monolayer N₂ on flat graphite was treated as a complement to previous studies of the melting of submonolayer commensurate N₂/graphite⁸ and for comparison with the present N₂/Ag(111) modeling. The following discussion is for the corresponding X1M model.²⁸

Using the onset of a van der Waals loop at nearly zero pressure as the criterion, the triple point temperature is bracketed by $27.5 < T_t < 30$ K. The calculated melting temperature for 0.5 commensurate monolayer of N₂/graphite is ~ 34 K,⁵ so the substrate corrugation does stabilize the solid to higher temperatures. The McLachlan energy for N₂/graphite is only 10% larger than for N₂/Ag(111), at given density, so that differences in tipping of molecular axes out of the monolayer plane may have some effect on the melting.

The melting temperature for 1.0 commensurate monolayer with this model is ~ 73 K.¹⁵ On flat graphite, a triangular lattice with $L = 4.26$ Å is under significant compression, as the unconstrained layer at 27.5 K has $L_u = 4.36$ Å. The melting transition of the 4.26 Å isochore of flat graphite occurs at 55–60 K and $\bar{\phi} \approx 20$ K/Å². That is, 60% of the temperature increase from 0.5 to 1.0 commensurate monolayer can be attributed directly to the pressure shift of the melting transition.

IV. DISCUSSION

The N₂/Ag(111) system appears to be an intrinsic planar molecular solid and thus is an important member of the fam-

ily of adsorbed molecular solids for establishing trends that depend on substrate corrugation. The inferred bulk modulus and the lattice constants of the observed orientationally disordered triangular lattice are in fair agreement with results of calculations for an interaction model with no corrugation but otherwise very similar to that used for N₂/graphite.

In a broader context, we have made quantitative predictions of phase transition temperatures starting from molecular models. The circumstances for N₂/Ag(111), where corrugation effects appear to be small, should enhance the accuracy of the modeling. Two immediate tests are available. (1) We find an onset of 2-in herringbone ordering²⁶ in a rectangular lattice distorted from a triangular center-of-mass lattice at temperatures a little below 20 K. It would be of great interest to confirm the shift from the 26–28 K transition temperature of N₂/graphite and the change in lattice symmetry as orientational ordering transitions have not yet been observed in two closely related cases, N₂/Cu(110) and N₂/MgO(001). (2) We predict that melting of the N₂/Ag(111) solid may be observed at temperatures of about 40 K if the 3D pressures can be held low enough that the unconstrained, nearly zero spreading pressure, solid is probed. Confirmation of the reduction in melting temperature from the 48 K of submonolayer N₂/graphite would provide support for the interpretation of incipient triple-point systems as having the solid preempting the liquid phase until the critical point is reached.

ACKNOWLEDGMENTS

This work has been partially supported by the National Science Foundation under Grant No. DMR-9423307 (L.W.B.) and by The Danish Natural Science Foundation (F.Y.H.). L.W.B. thanks the Department of Chemistry and the Technical University of Denmark for hospitality during the period this work was begun. We thank the authors of Refs. 3 and 7 for prepublication copies of their work.

¹T. A. Scott, Phys. Rep. **27**, 89 (1976) and references contained therein.

²L. W. Bruch, M. W. Cole, and E. Zaremba, *Physical Adsorption: Forces and Phenomena* (Oxford University Press, New York, 1997).

³G. S. Leatherman and R. D. Diehl, Langmuir **13**, 7063 (1997).

⁴D. Marx and H. Wiechert, Adv. Chem. Phys. **95**, 213 (1997).

⁵F. Y. Hansen, L. W. Bruch, and H. Taub, Phys. Rev. B **52**, 8515 (1995).

⁶M. Trabelsi, J. P. Coulomb, D. Degenhardt, and H. Lauter, Surf. Sci. **377–379**, 38 (1997).

⁷P. Zeppenfeld, J. Goerge, V. Diercks, R. Halmer, R. David, G. Comsa, A. Marmier, C. Ramseyer, and C. Girardet, Phys. Rev. Lett. **78**, 1504 (1997); A. Marmier, C. Ramseyer, P. N. M. Hoang, C. Girardet, J. Goerge, P. Zeppenfeld, M. Büchel, R. David, and G. Comsa, Surf. Sci. **383**, 321 (1997).

⁸F. Y. Hansen, L. W. Bruch, and H. Taub, Phys. Rev. B **54**, 14 077

(1996) and references contained therein.

⁹A. C. Kummel, G. O. Sitz, R. N. Zare, and J. C. Tully, J. Chem. Phys. **89**, 6947 (1988).

¹⁰The calculated binding energy of 69 meV reported in Ref. 9 was obtained by summing over only the topmost layer of Ag atoms; the corresponding value of ω_{\perp} is 4.4 meV. The sum is done for two layers in the present work in order to bring the monolayer energy closer to the experimental value (Ref. 3) of 103 meV and thus to reduce the possibility of nonwetting introduced by an artificially weak substrate binding.

¹¹F. Y. Hansen, V. L. P. Frank, H. Taub, L. W. Bruch, H. J. Lauter, and J. R. Dennison, Phys. Rev. Lett. **64**, 764 (1990).

¹²J. Cui, D. R. Jung, and R. D. Diehl, Phys. Rev. B **45**, 9375 (1992); R. Vollmer, Ph.D. thesis, University of Göttingen, 1991 (unpublished); K. D. Gibson and S. J. Sibener, J. Chem. Phys. **88**, 7862 (1988).

¹³M. Gruyters and K. Jacobi, Chem. Phys. Lett. **225**, 309 (1994).

- ¹⁴W. A. Steele, *Interaction of Gases with Solid Surfaces* (Pergamon, Oxford, 1974).
- ¹⁵F. Y. Hansen and L. W. Bruch, *Phys. Rev. B* **51**, 2515 (1995).
- ¹⁶S. E. Roosevelt and L. W. Bruch, *Phys. Rev. B* **41**, 12 236 (1990).
- ¹⁷M. P. Allen and D. J. Tildesley, *Computer Simulation of Liquids* (Oxford University Press, New York, 1987), Sec. 2.4; J. Alejandro, D. J. Tildesley, and G. A. Chapela, *J. Chem. Phys.* **102**, 4574 (1995).
- ¹⁸For instance, for the Ag models at 15 K, without the McLachlan term the triangular lattice with $L=4.16$ Å has $\phi_{xx}=-0.8$ and $\phi_{yy}=1.4$ K/Å² and with that term, the triangular lattice with $L=4.21$ Å has $\phi_{xx}=-1.2$ and $\phi_{yy}=2.6$ K/Å².
- ¹⁹For spherical adsorbates, see H.-Y. Kim and W. A. Steele, *Phys. Rev. B* **45**, 6226 (1992).
- ²⁰B. Kuchta and R. D. Etters, *Phys. Rev. B* **54**, 12 057 (1996).
- ²¹V. R. Bhethanabotla and W. A. Steele, *Langmuir* **3**, 581 (1987).
- ²²That the classical-limit quasiharmonic approximation gives a larger molar area than the molecular-dynamics result is probably a consequence of an incipient failure of the quasiharmonic approximation. The failure arises through an artificial dilation of the lattice, to the point of dynamical instability, to lower the free energy by lowering the harmonic frequencies. In this case, a local minimum in the free energy is still found at 20 K but not at 21 K.
- ²³T. Angot, Ph.D. Thesis, Université D'Aix Marseille II, 1991 (unpublished).
- ²⁴M. T. Alkhafaji, P. Shrestha, and A. D. Migone, *Phys. Rev. B* **50**, 11 088 (1994); A. D. Migone (private communication).
- ²⁵K. Morishige, K. Inoue, and K. Imai, *Langmuir* **12**, 4889 (1996).
- ²⁶This terminology follows A. B. Harris and A. J. Berlinsky, *Can. J. Phys.* **57**, 1852 (1979). The 2-in herringbone is a two-sublattice structure with two glide planes and the molecular axes parallel to the adsorption plane.
- ²⁷To estimate the reliability of the estimated transition temperature for N₂/Ag(111), consider the results for commensurate N₂/graphite, where the transition is known to occur at 26–28 K. The methods were previously applied (Ref. 15) to the graphite X1M case and gave a transition temperature of 22–23 K. Repeating those calculations with the X1 model gives very similar results. The uncertainty in determining the transition temperature is larger than the differences between the two sets of $S(1,2)$ data. Thus, the estimated transition temperature for N₂/Ag(111) may be low by about 5 K.
- ²⁸Qualitative aspects of nitrogen on flat graphite were explored, with a different interaction model, by J. Talbot, D. J. Tildesley, and W. A. Steele, *Mol. Phys.* **51**, 1331 (1984). In particular they found that a submonolayer patch on smooth graphite at 16 K dilates and distorts from the commensurate structure.